Azaadamantyl Nitroxide Spin Label: Complexation with β-Cyclodextrin and Electron Spin Relaxation

Sandra S. Eaton,[a]* Andrzej Rajca,[b] Zhimin Yang,[b] and Gareth R. Eaton[a]

[a]*Department of Chemistry and Biochemistry, University of Denver, Denver, Colorado 80210-2436, United States;* [b]*Department of Chemistry, University of Nebraska, Lincoln, Nebraska 68588-0304, United States*

The authors have no financial conflicts of interest.

Azaadamantyl Nitroxide Spin Label: Complexation with β-Cyclodextrin and Electron Spin Relaxation

An iodoacetamide azaadamantyl spin label was studied in fluid solution and in 9:1 trehalose:sucrose glass. In 9:1 toluene:CH_2Cl_2 solution at 293 K the isotropic nitrogen hyperfine coupling is 19.2 G, T_1 is 0.37 μs and T_2 is 0.30 to 0.35 μs. Between about 80 and 150 K $1/T_m$ in 9:1 trehalose:sucrose is approximately independent of temperature demonstrating that the absence of methyl groups decreases $1/T_m$ relative to that which is observed in spin labels with methyl groups on the alpha carbons. Spin lattice relaxation rates between about 80 and 293 K in 9:1 trehalose:sucrose are similar to those observed for other nitroxide spin labels, consistent with the expectation that relaxation is dominated by Raman and local mode processes. Although complexation of the azaadamantyl spin label with β-cyclodextrin slows tumbling in aqueous solution by about a factor of 10, it has little impact on $1/T_1$ or $1/T_m$ in 9:1 trehalose:sucrose between 80 and 293 K.

Keywords: double electron electron resonance, spin lattice relaxation, spin echo dephasing,

Introduction

Nitroxide radicals are widely used as spin labels and can be incorporated into biomolecules at desired locations introduced by site-directed mutagenesis [1]. Double electron-electron resonance (DEER) is a powerful method to determine distances between pairs of nitroxide labels in the range of 1.5 to 8 nm [2]. Currently most DEER experiments with nitroxide radicals are performed at temperatures between 50 and 70 K with expensive liquid helium or with poorer signal-to-noise at 80 K with less-expensive liquid nitrogen. The experiments are based on observation of an electron spin echo. Longer times between the pulses that form the

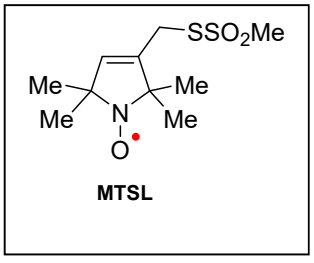

MTSL

echo permits measurement of longer interspin distances. As the time between the pulses is increased, the intensity of the echo decreases exponentially with a time

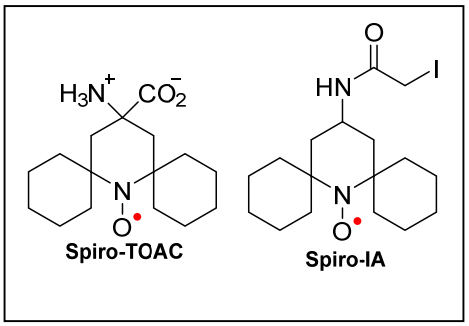

constant T_m. Longer values of T_m permit data acquisition with better signal-to-noise, improved definition of distributions of interspin distances, and the opportunity to measure longer interspin distances. Nitroxides such as MTSL that are currently used for most DEER experiments have gem-dimethyl groups on the alpha carbons adjacent to the N-O moiety. At temperatures above about 80 K these methyls rotate at rates that are comparable to the anisotropy in the electron-proton hyperfine interactions which increases $1/T_m$ and makes DEER experiments impractical [3]. There is substantial interest in nitroxides that have groups other than methyls on the alpha carbons. Bulky groups on the alpha carbons are required for the stability of the nitroxides.

Nitroxides with spirocyclohexyl groups on the alpha carbons (spiro-TOAC) demonstrated that replacement of the methyl groups decreased $1/T_m$ above 80 K in rigid glassy matrices [3]. Double spin labeling of T4 lysozyme with spiro-IA and immobilization in a trehalose glass permitted DEER measurement of an interspin distance of 3.2 nm at room temperature [4]. Spirocyclohexyl groups are relatively bulky and hydrophobic so they are not optimal for attachment to biomolecules. Although there are methyl groups in the substituents on the alpha carbons of spin labels

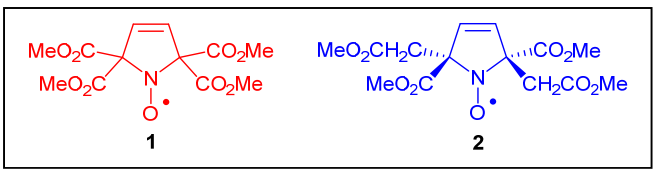

1 and **2**, the hyperfine couplings to these remote protons are much smaller than for the directly-bound methyls of MTSL so rotation of the methyl groups in **1** or **2** have much

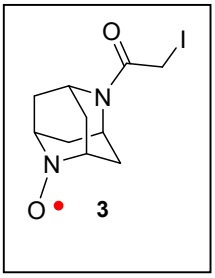

less impact on spin echo dephasing than the methyls of MTSL [5]. As a further step in characterizing spin labels without methyl groups, the azaadamantyl spin label **3** has been prepared. This paper reports the electron spin relaxation properties of **3** in fluid solution and in 9:1 trehalose:sucrose glass and of the complex of **3** with β-cyclodextrin in 9:1 trehalose:sucrose glass.

Methods and Materials

The synthesis of azaadamantyl spin label **3** will be reported separately. Solutions of **3** in water were in 1 mm ID pyrex capillaries and were air saturated. To permit rigorous degassing, a 0.2 mM solution of **3** in 9:1 toluene:CH_2Cl_2 was prepared. A sample in a 4 mm OD quartz EPR tube was degassed by multiple cycles of freeze-pump-thaw and flame sealed.

D(+)-trehalose (Sigma-Aldrich, St. Louis, MO) and β-cyclodextrin (Sigma-Aldrich) were used as received. The preparation of 9:1 trehalose:sucrose glasses was performed as reported previously [5] with a 2000:1 molar ratio of sugars to **3**. The addition of sucrose to the trehalose enhances glass formation. The initial concentrations were 0.09 M trehalose, 0.01 M sucrose, and 0.05 mM **3**. To form the β-cyclodextrin complex in the sugar glass solid was added to the initial solution to make a 3.2 mM β-cyclodextrin solution. The concentrations of all solutes increase as the water evaporates. After the glasses were formed by slow evaporation of the water, the glassy solids were scraped off the glass surface and transferred to 4 mm OD quartz EPR tubes. Samples were evacuated overnight on a high vacuum line to remove oxygen and residual water and then flame sealed. Handling of **3** and its samples was performed with minimum lighting to avoid photodegradation.

CW EPR

CW spectra were recorded on a Bruker X-band EMX spectrometer with an SHQE resonator. Simulations of fluid solution and rigid lattice spectra were performed with locally-written software that calculates hyperfine splittings to first order. Hamiltonian parameters are summarized in Tables 1 and 2.

Pulsed EPR

Pulsed EPR spectra and relaxation times were recorded at X-band on a Bruker E580 spectrometer with an ER4118X-MS5 split ring resonator. The length of a 90^{o} pulse was 40 ns. T_m in rigid lattice and T_2 in fluid solution were measured by two-pulse echo decay with a $\pi/2$ - τ - π - τ - echo sequence, initial τ = 200 ns, and 2-step phase cycling. Field-swept echo-detected spectra were obtained with a $\pi/2$ - τ - π - τ - echo sequence and a constant τ = 120 ns, unless specified otherwise. T_1 was measured by inversion recovery with a π- T- $\pi/2$ - τ - π - τ - echo sequence, a constant τ = 360 ns, variable T, and 2-step phase cycling. The temperature dependence of relaxation was monitored at the magnetic field that corresponds to the maximum in the absorption spectrum, which is near the center of the spectrum. This position corresponds predominantly to molecules for which the magnetic field is in the molecular xy plane. Echo decays and inversion recovery curves were fitted with single exponentials.

Results and Discussion

Fluid solution

The X-band spectrum of 0.2 mM **3** in deoxygenated 9:1 toluene:CH_2Cl_2 is shown in Figure 1. On each nitrogen hyperfine line there is well-resolved proton hyperfine splitting. Decreasing the modulation amplitude and microwave power below the values used to record the spectrum in Figure 1A did not decrease the linewidth. The simulations of the spectra were obtained with the hyperfine coupling constants listed in Table 1 and a peak-to-peak linewidth of 0.57 G. The nitrogen hyperfine coupling of 19.2 G for **3** is significantly larger than the 15 to 16 G that is typical for a many nitroxides [6] and much larger than the A_N = 12.2 G for **1** or 13.4 G for **2** in $CHCl_3$. The resolved hyperfine splittings include the two protons on the nearest bridgehead carbons, inequivalent couplings to the two protons of each of the four CH_2 groups and either the protons on the distant bridgehead carbons or the distant nitrogen. That leaves either the distant nitrogen or the protons on the distant bridgehead carbons as unresolved contributions to the linewidths. Rassat and co-workers prepared the closely-related radical **4** as a precursor to a diradical and commented on the extensive well-resolved hyperfine splitting [7]. They assigned the hyperfine couplings based on the symmetry of the molecule and by integration of the peaks in the paramagnetic NMR spectrum. The hyperfine couplings in toluene:CH_2Cl_2 are significantly different than in H_2O (Table 1) which is consistent with the frequently observed dependence of nitroxide hyperfine splittings on solvation [8, 9, 10].

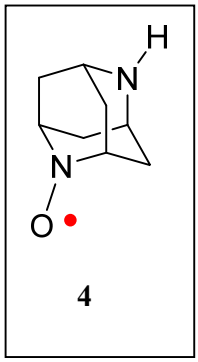

4

Relaxation in Fluid solution

The field-swept echo-detected spectrum of **3** in 9:1 toluene:CH_2Cl_2 (Figure 2B) is in good agreement with the first integral of the CW spectrum (Figure 2A). The primary difference is the reduced amplitude of the high-field line in the echo-detected spectrum, which occurs because the smaller T_2 for that hyperfine manifold has greater impact on the echo-detected spectrum than on the CW spectrum. The values of T_1 and T_2 for the three nitrogen hyperfine manifolds are summarized in Table 3. The observation of $T_1 \sim T_2$ is characteristic of nitroxides near the rapid tumbling limit [11]. The nitrogen m_I dependence of T_2 reflects the residual contribution from incomplete motional averaging of g- and A-anisotropy. Application of the Kivelson model to the m_I dependence of T_2 [12, 13] and the anisotropic g and A values for **3** (Table 2) gave a tumbling correlation time, τ_R, of 10 ± 3 ps. The dependence of T_1 on nitrogen $m_I = -1 > m_I = 0 > m_I = +1$ is consistent with prior observations for rapidly tumbling nitroxides at about this concentration [14]. In fluid solution the spin lattice relaxation mechanisms for nitroxides are strongly dependent on τ_R [11]. The τ_R for **3** in toluene:CH_2Cl_2 is similar to that for tempone in H_2O (9 ps). For 0.25 mM tempone in deoxygenated water T_1 is 0.59 μs [14]. A major contribution to $1/T_1$ for rapidly tumbling nitroxides is the modulation of nitrogen hyperfine anisotropy [11, 14, 15]. For about the same τ_R the shorter T_1 (faster $1/T_1$) for **3** than for tempone may be due in part to the larger nitrogen hyperfine couplings for **3**.

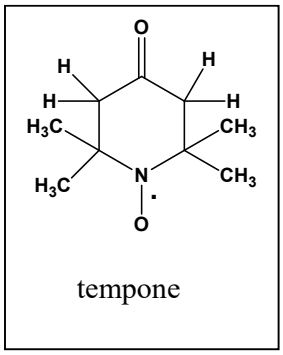

tempone

The relationship between T_2 and ΔB_{pp} for a Lorentzian line is given by Eq. (1)

$$\Delta B_{pp} = \frac{2}{\sqrt{3}\gamma T_2} = \frac{6.56x10^{-8}\ \mathrm{G}}{\mathrm{T}_2} \qquad (1)$$

Using Eq. (1) and the values of T_2 in Table 2, spin-spin relaxation contributes 0.19 to 0.22 G to the CW linewidths for **3** in fluid solution. These values are substantially smaller that the experimental linewidth of 0.57 G, consistent with additional contributions to the linewidths from unresolved nuclear hyperfine splitting.

Complexation with β-cyclodextrin

Cyclodextrins are polymers of D-glucopyranose with hydrophobic cavities that form inclusion complexes with a wide range of small molecules including nitroxides [16, 17, 18] and adamantyl groups [19, 20, 21]. Complexation of **3** with β-cyclodextrin was examined as a method of decreasing mobility. The spectrum of 1.0 mM **3** in water at room temperature is shown in Figure 3A. Addition of 18 mM β-cyclodextrin (18:1 molar ratio) causes substantial broadening of the high-field nitrogen hyperfine line (Figure 3B), which is characteristic of slower tumbling [22]. Simulations indicate that proton hyperfine splitting is not resolved on the high-field line of spectrum for the slowly tumbling β-cyclodextrin complex. The low amplitude sharp hyperfine lines that are superimposed on the broad high-field line (Figure 3A) are attributed to a few percent of **3** that is not bound to β-cyclodextrin Since the 18:1 mole ratio resulted in essentially complete conversion to the complex in water solution, the 60:1 mole ratio of β-cyclodextrin to **3** that was used in preparation of the trehalose:sucrose glass should ensure essentially complete complex formation. The nitrogen hyperfine coupling is reduced from 19.2 G for **3** to 18.6 G for the β-cyclodextrin complex. The dependence of linewidths on nitrogen m_I was analysed using the Kivelson model [12] to obtain τ_R = 15 ± 3 ps for **3** in water, and τ_R = 175 ± 25 ps for the β-cyclodextrin complex.

Spectra of immobilized samples in 9:1 trehalose:sucrose

Lineshapes

The CW spectrum of **3** complexed to β-cyclodextrin in 9:1 trehalose:sucrose at 293 K is shown in Figure 4E and is similar to that for **3** (data not shown). The Hamiltonian parameters obtained by simulation of the spectra are in Table 2, along with the values reported previously for **1** and **2** in 9:1 trehalose:sucrose [5]. These g values are similar to those for a wide range of nitroxides [8, 23, 24, 25]. A distinctive feature for **3** is the larger values of A_x A_y, which are the dominant contribution to the larger value of the isotropic A value that is observed in fluid solution.

Temperature dependence of spin relaxation

The spin lattice relaxation rate, $1/T_1$, determines how rapidly the signal averaging for the DEER experiment can be performed. The temperature dependence of $1/T_1$ and $1/T_m$ for **1**, **2**, **3**, and **3** complexed to β-cyclodextrin are similar (Figure 5), indicating that the underlying relaxation mechanisms are the same. The similarity in $1/T_1$ for the four samples is consistent with the expectation that relaxation in the temperature range studied is dominated by the Raman process and a local mode [26, 27]. These processes modulate spin-orbit coupling [26]. Spin-orbit coupling also is reflected in deviations of g values from the free electron value. Since g values are similar for many nitroxides, electron spin relaxation in the same host lattice also is expected to be similar [27]. Between about 80 and 293 K $1/T_1$ is slightly faster for **3** and for its β-cyclodextrin complex than for **1** or **2**. In glassy matrices smaller nitroxides relax faster than larger nitroxides which may be due to differences in mobility [27]. This analogy suggests that weaker interaction between the nonpolar adamantyl fused ring structure and the trehalose:sucrose lattice than for **1** or **2** may contribute to faster spin lattice relaxation

for **3** than for **1** or **2**. Complexation of **3** to β-cyclodextrin had negligible impact on $1/T_1$ in the sugar glass. Between 80 and 140 K $1/T_m$ is approximately independent of temperature, but is faster for **3** complexed to β-cyclodextrin than for **3** alone, which suggests that there may be motional process for the complex that contributes to relaxation. At 80 to 293 K, $1/T_m$ is faster for both **3** and for **3** complexed to β-cyclodextrin than for either **1** or **2**, which again suggests increased motion.

The dominant contributions to $1/T_m$ at 80 to 293 K for samples in glassy matrices are motions that move the spins off resonance on the microsecond timescale of the spin echo experiment. The impact of these motions can be seen by comparing the field-swept echo-detected spectra in Figure 4. In a field-swept echo-detected spectrum the amplitude of the signal at a particular position in the spectrum is determined by the number of spins on resonance and by $1/T_m$ for those spins. If $1/T_m$ is independent of position in the spectrum, the field-swept echo detected spectrum is the same as the first integral of the CW spectrum. For the β-cyclodextrin complex of **3** at 80 K the field-swept echo detected spectrum (Figure 4C) is similar to the first integral of the CW spectrum at 293 K (Figure 4E). At 293 K and τ = 120 ns (Figure 4B) there is a conspicuous decrease in echo intensity at about 3340 G and between about 3380 and 3400 G. These differences become even greater for τ = 600 ns. Larger values of the constant time τ in the two-pulse experiment provide more time for the spins to dephase, which accentuates the effects of differences in $1/T_m$ across the spectrum.

The variation in $1/T_m$ across the spectrum for **3** in 9:1 trehalose:sucrose at 293 K is shown in Fig. 6. The slowest dephasing rates are near 3370 G, which is near the resonance positions for nitrogen $m_I = 0$ and a wide range of orientations of the molecule with respect to the magnetic field. For these molecules motion has little impact on the

resonance position and low amplitude motions cause little dephasing. The resonance for nitrogen $m_I = -1$ and the magnetic field along the molecular z axis occurs at about 3335 G. For $m_I = -1$ and other orientations of molecule with respect to the external field resonance occurs between about 3335 and 3355 G. Resonance is less sensitive to motion for molecules for which the magnetic field is aligned with the z axis and more sensitive for intermediate orientations [28] which is why $1/T_m$ is slower near 3335 G than at intermediate fields. For nitrogen $m_I = +1$ and the magnetic field along the molecular z axis occurs at about 3410 G, but for other orientations the resonance occurs between about 3370 and 3410 G. For these intermediate orientations of the molecule with respect to the external field, even small changes in orientation result in substantial changes in resonance field, which causes very effective dephasing. The larger values of $1/T_m$ between about 3380 and 3405 G result in large decreases in amplitude of the echo detected spectrum when τ is 600 ns at 293 K (Figure 5A).

The similarity in values of $1/T_m$ for **3** and for its complex with β-cyclodextrin suggests that complexation has little impact on the low amplitude motions that impact $1/T_m$. The slower values of $1/T_m$ for **1** and **2** than for **3** at 293 K indicate that there is less mobility of the carboxymethyl substituted nitroxides than for the adamantyl nitroxide. The polar carboxymethyl groups may interact more strongly with the trehalose:sucrose lattice than the relatively non-polar adamantyl group.

Summary

There are no methyl groups in the azaadamantyl spin label which removes the contribution to spin echo dephasing from rotation of methyl groups that are present in widely used spin labels including MTSL. For the azaadamantyl spin label in 9:1 trehalose:sucrose glass $1/T_m$ is weakly dependent on temperature up to about 150 K, as

predicted for a nitroxide without methyl groups that are strongly spin-coupled to the nitroxide. The g values for the azaadamantyl nitroxide are similar to those for other nitroxides, which indicates that spin orbit coupling is similar. The temperature dependence of $1/T_1$ is similar to that for other nitroxides, consistent with the expectation that spin lattice relaxation is dominated by processes that modulate spin-orbit coupling. Although complexation with β-cyclodextrin has a large impact on the tumbling correlation time for **3** in aqueous solution, it has little impact on $1/T_1$ or $1/T_m$ in a 9:1 trehalose:sucrose glass at 80 to 293 K.

Acknowledgements.

Financial support from NIH [R01 CA177744] to GRE and SSE, NIH [R01 EB019950] to AR and SSE, NIH [R01 GM124310] to AR and SSE, and NSF [CHE-1665256] to AR is gratefully acknowledged.

Table 1

Nuclear hyperfine coupling constants (in G)

	N	2 H	4H	4H
3 in 9:1 tol:CH_2Cl_2[a]	19.2	2.45	1.60	0.60
3 in H_2O	19.2	2.80	1.45	0.80
4 in H_2O [b]	19.2	2.80	1.45	0.80

[a] Used in the simulation shown in Figure 1. In addition to the hyperfine couplings listed in this Table a coupling of about 0.60 G to two equivalent protons or 1 additional nitrogen is needed to account for the full extent of the spectrum.

[b] Reported in ref. [7]

Table 2

Hamiltonian parameters for nitroxides in 9:1 trehalose:sucrose

	g_{xx}	g_{yy}	g_{zz}	A_{xx} (G)	A_{yy} (G)	A_{zz} (G)	Ref.
1	2.0099	2.0060	2.0025	3.4	3.5	29.7	[5]
2	2.0099	2.0061	2.0026	4.2	4.3	31.8	[5]
3	2.0095	2.0062	2.0025	7.4	12.8	37.4	
3 + β-cyclodextrin	2.0095	2.0062	2.0027	7.4	11.7	35.6	

Table 3

Electron Spin Relaxation Times (μs) of **3** in 9:1 toluene:CH_2Cl_2 at 293 K

Nitrogen hyperfine line[a]	$m_I = -1$	$m_I = 0$	$m_I = 1$
T_1 (μs)[b]	0.39	0.37	0.36
T_2 (μs)[b]	0.35	0.34	0.30

[a] $m_I = -1$ is the low-field nitrogen hyperfine line.

[b] Uncertainties in T_1 and T_2 are about 5%.

References

1. Hubbell WL, Lopez CJ, Altenbach C, et al. Technological advances in site-directed spin labeling of proteins. Current Topics Structural Biology. 2013;23:725 - 733

2. Jeschke G. DEER Distance Measurements on Proteins. Annu Rev Phys Chem. 2012;63:419 - 446.

3. Rajca A, Kathirvelu V, Roy SK, et al. A spirocyclohexyl nitroxide amino acid spin label for pulsed EPR spectroscopy distance measurements. Chem Eur J. 2010;16:5778 - 5782.

4. Meyer V, Swanson MA, Clouston L, et al. Room-Temperature Distance Measurements of Immobilized Spin-Labeled Protein by DEER/PELDOR. Biophysical J. 2015;108:1213 – 1219

5. Huang S, Paletta JT, Elajaili H, et al. Synthesis and Electron Spin Relaxation of Tetra-Carboxylate Pyrroline Nitroxides J Org Chem. 2017;82:1538 - 1544.

6. Rockenbauer A, Gyor M, Hankovszky HO, et al. ESR of the conformation of 5- and 6-membered cyclic nitroxide (aminoxyl) radicals. Electron Spin Resonance. 1988;11A:145-182.

7. Dupeyre R-M, Rassat A, Ronzaud J. Electron Spin Resonance Studies of N,N'-Dioxy-2,6-diazaadamantane, a Symmetrical Ground State Triplet. J Amer Chem Soc. 1974;96:6559 - 6568.

8. Berliner LJ. Compilation of Hyperfine Splittings and g-Factors for Aminoxyl (Nitroxide) Radicals. In: Misra SK, editor. Multifrequency Electron Paramagnetic Resonance. Weinheim, Germany Wiley-VCH; 2014. p. 287 - 296.

9. Morrisett JD. The Use of Spin Labels for Studying the Structure and Function of Enzymes. 1976. In: Spin Labeling Theory and Applications [Internet]. New York: Academic Press; [307].

10. Bales BL. Inhomogeneously Broadened Spin-Label Spectra. Biol Magn Reson. 1989;8:86 - 87

11. Biller JR, Elajaili H, Meyer V, et al. Electron Spin Lattice Relaxation Mechanisms of Rapidly-Tumbling Nitroxide Radicals. J Magn Reson. 2013;236:47 - 56.

12. Wilson R, Kivelson D. ESR linewidths in solution. IV. Experimental studies of anisotropic and spin-rotation effects in copper complexes. J Chem Phys. 1966;44:4445-4452.

13. Chasteen ND, Hanna MW. Electron Paramagnetic Resonance Line Widths of Vanadyl (IV) α-hydroxycarboxylates. J Phys Chem. 1972;76:3951-3958.

14. Biller JR, Meyer V, Elajaili H, et al. Relaxation Times and Line Widths of Isotopically-Substituted Nitroxides in Aqueous Solution at X-band. J Magn Reson. 2011;212:370-377.

15. Mailer C, Nielsen RD, Robinson BH. Explanation of Spin-Lattice Relaxation Rates of Spin Labels Obtained with Multifrequency Saturation Recovery EPR. J Phys Chem A. 2005;109:4049-4061.

16. Strizhakov RK, Tretyakov EV, Medvedeva AS, et al. Permethyl-β-Cyclodextrin Spin-Labeled with Nitronyl Nitroxide: Synthesis and EPR Study. Appl Magn Reson. 2014;45:1087- 1098.

17. Bardelang D, Casano G, Poulhes F, et al. Spin Exchange Monitoring of the Strong Positive Homotropic Allosteric Binding of a Tetraradicals by a Synthetic Receptor in Water. J Amer Chem Soc. 2014;136:17570 - 17577.

18. Ionita G, Caragheorgheopol A, Caldararu H, et al. Inclusion complexes of cyclodextrins with nitroxide-based spin probes. Org Biomol Chem. 2009 7:598 - 602.

19. Dzikovski B, Tipikin DS, Livshits V, et al. Multifrequency ESR study of spin-labeled molecules in inclusion compounds with cyclodextrins. Phys Chem Chem Phys. 2009;11:6676 - 6688.

20. Car Z, Kodrin I, Pozar J, et al. Experimental and computational study of the complexation of adamantyl glycosides with β-cyclodextrin. Tetrahedron. 2013;69:8051 - 8063.

21. Wang J, Xu Y, Wang Y, et al. Bridged-cyclodextrin supramolecular hydrogens: host-guest interaction between a cyclodextrin dimer and adamantyl substituted poly(acrylate)s. RSC Adv. 2015;5:46067 - 46073.

22. Freed JH. Theory of slow tumbling ESR spectra of nitroxides. In: Berliner LJ, editor. Spin Labeling: Theory and Applications. New York: Academic Press; 1976. p. 53-132.

23. Freed JH. Theory of Slow Tumbling ESR Spectra for Nitroxides. 1976. In: Spin Labeling Theory and Applications [Internet]. New York: Academic Press; [73 - 75].

24. Berliner LJ. Principal Values of the g and Hyperfine Tensors for Several Nitroxides Reported to Date. In: Berliner LJ, editor. Spin Labeling Theory and Applications. New York Academic Press; 1976. p. 564 -565.

25. Yamauchi J. Fundamentals of Electron Spin Resonance (ESR). Nitroxides. Weinheim, Germany: Wiley-VCH; 2008. p. 96.

26. Eaton SS, Eaton GR. Relaxation times of organic radicals and transition metal ions. Biol Magn Reson. 2000;19:29-154. PubMed PMID: An 2001:633666.

27. Sato H, Kathirvelu V, Fielding AJ, et al. Impact of molecular size on electron spin relaxation rates of nitroxyl radicals in glassy solvents between 100 and 300 K. Mol Phys. 2007;105:2137-2151.

28. Du JL, More KM, Eaton SS, et al. Orientation dependence of electron spin phase memory relaxation times in copper(II) and vanadyl complexes in frozen solution. Israel J Chem. 1992;32:351-5. PubMed PMID: An 1993:419034.

Figure Captions

Figure 1. CW spectra (9.866 GHz) at 293 K of 0.2 mM **3** in deoxygenated 9:1 toluene:CH_2Cl_2 recorded with 0.5 mW microwave power and 0.05 G modulation amplitude at 100 kHz. A) Full spectrum. B) Spectrum of nitrogen $m_I = 0$ line. Simulations obtained with the parameters listed in Table 1 are shown with dashed (red) lines.

Figure 2. Absorption spectra of 0.2 mM **3** at 293 K in deoxygenated 9:1 toluene:CH_2Cl_2. A) First integral of CW spectrum shown in Figure 1A. B) Field-swept echo detected spectrum obtained with $\pi/2$ pulse lengths of 120 ns, constant two-pulse spacing of 200 ns, and integration of the echo intensity starting at the peak and extending for 400 ns.

Figure 3. CW spectra (9.868 GHz) in H_2O at 293 K recorded with 2.0 mW microwave power and 0.10 G modulation amplitude at 100 kHz. A) 1.0 mM **3**. B) 1.0 mM **3** plus 18 mM β-cyclodextrin.

Figure 4. Spectra of **3** at 9.337 GHz complexed with β-cyclodextrin in 9:1 trehalose:sucrose. A) Field-swept echo detected spectrum at 293 K obtained with a constant two-pulse spacing of 600 ns. B) Field-swept echo detected spectrum at 293 K obtained with a constant two-pulse spacing of 120 ns. C) Field-swept echo detected spectrum at 80 K obtained with a constant two-pulse spacing of 120 ns. D) First integral of CW spectrum at 293 K. E) CW spectra at 293 K and simulation (red dashed line) obtained with the parameters in Table 3.

Figure 5. Temperature dependence of $1/T_1$ at X-band (9.46 GHz) in the perpendicular plane (blue circles) **1**, (red squares) **2**, (green diamonds) **3**, (black x) **3** plus β-cyclodextrin. Temperature dependence of $1/T_m$ at X-band in the perpendicular plane

(blue triangles) **1**, (red plus) **2**, (green inverted triangles) **3**, (black sidewise triangles) **3** plus β-cyclodextrin. Lines connect the data points. Samples were in 9:1 trehalose:sucrose. Data for **1** and **2** are reproduced from Ref. [5].

Figure 6. A. Orientation dependence of $1/T_m$ in 9:1 trehalose:sucrose. (black diamonds) **3**, (green +) **3** plus cyclodextrin and two comparison points for (red circles) **1**, and (blue triangles) **2**. B. Field - swept echo detected spectrum for **3** plus cyclodextrin at 293 K in 9:1 trehalose:sucrose obtained with constant two-pulse echo spacing of 120 ns. Approximate positions of the extrema for nitrogen m_I = -1, 0, +1 along the x, y, and z axes are marked below the spectrum.

Figure 1.

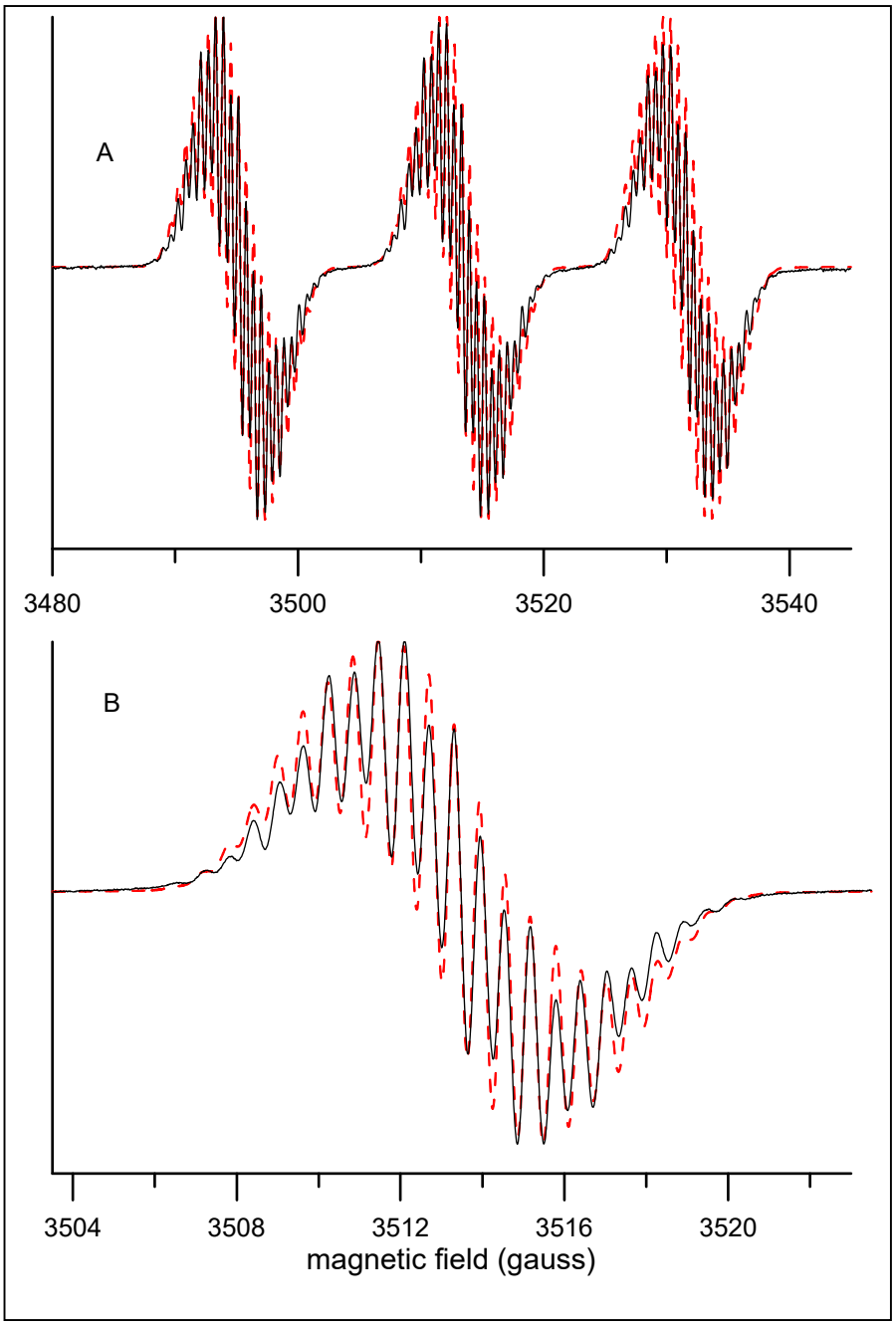
A
3480
3500
3520
3540
B
3504
3508
3512
3516
3520
magnetic field (gauss)

Figure 2.

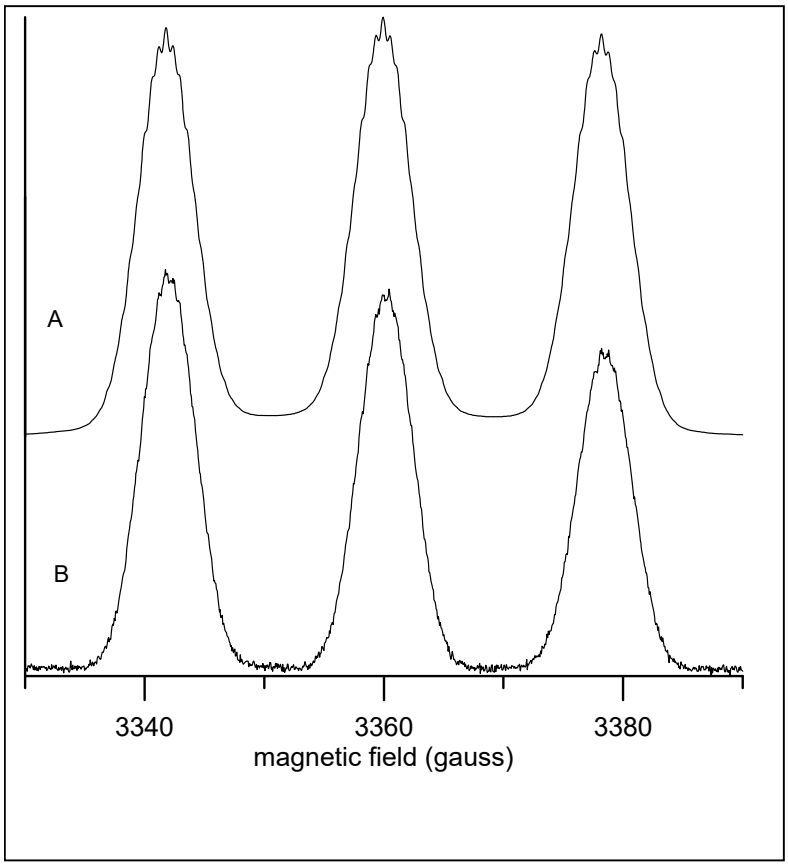

Figure 3.

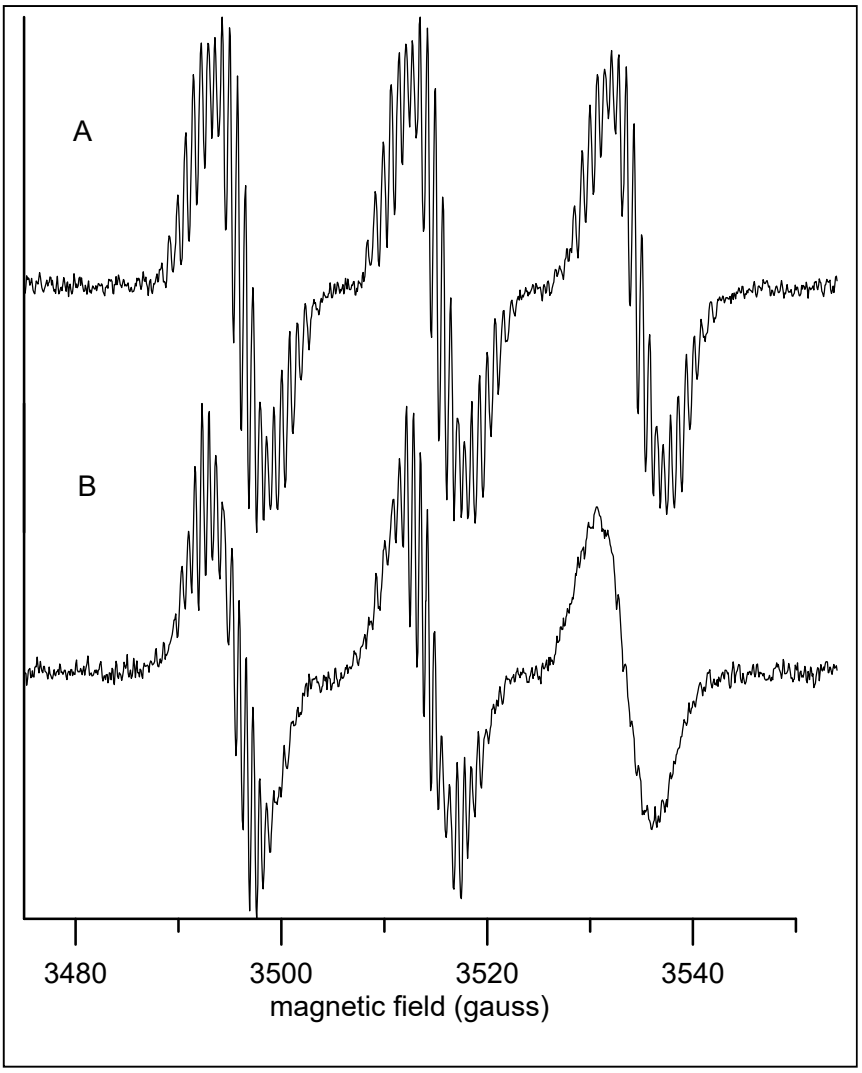

Figure 4.

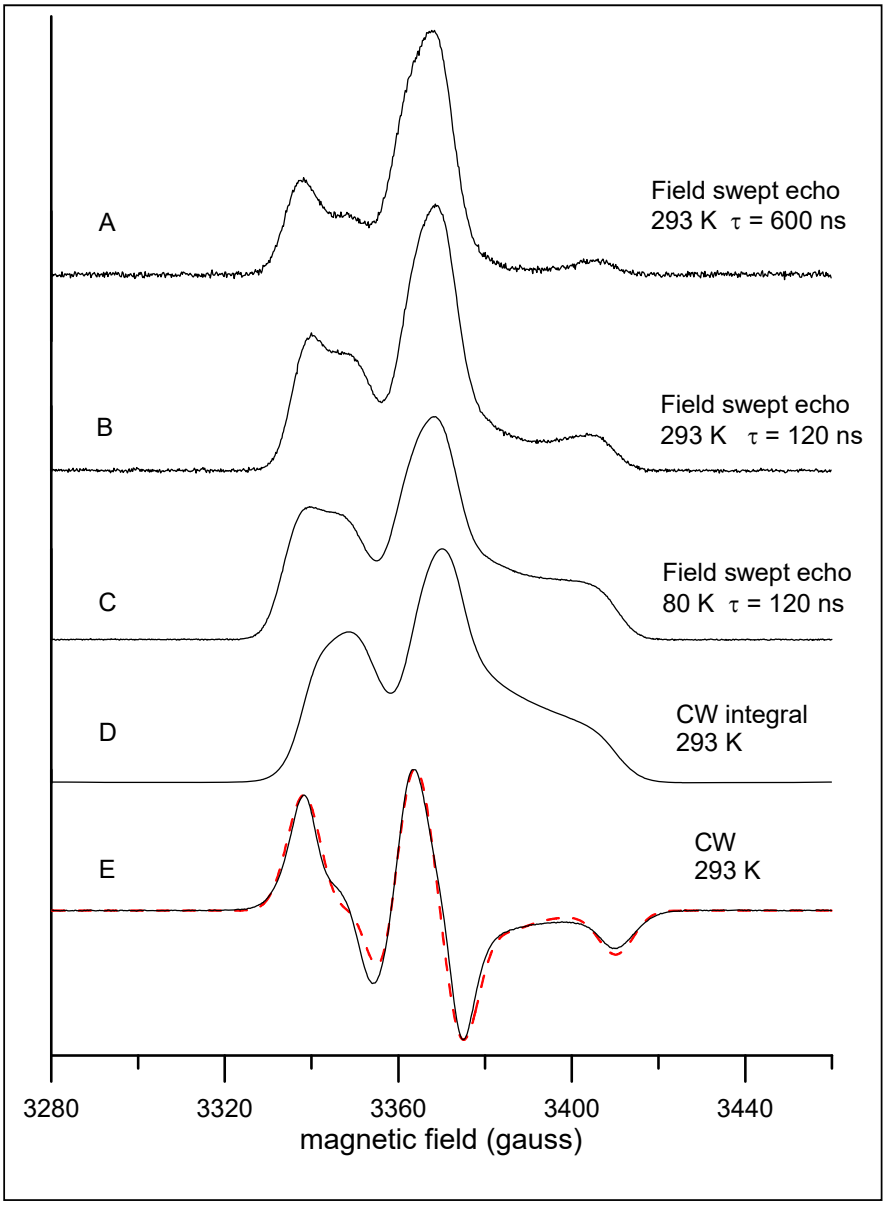
A
Field swept echo
293 K τ = 600 ns
B
Field swept echo
293 K τ = 120 ns
C
Field swept echo
80 K τ = 120 ns
D
CW integral
293 K
E
CW
293 K
3280
3320
3360
3400
3440
magnetic field (gauss)

Figure 5.

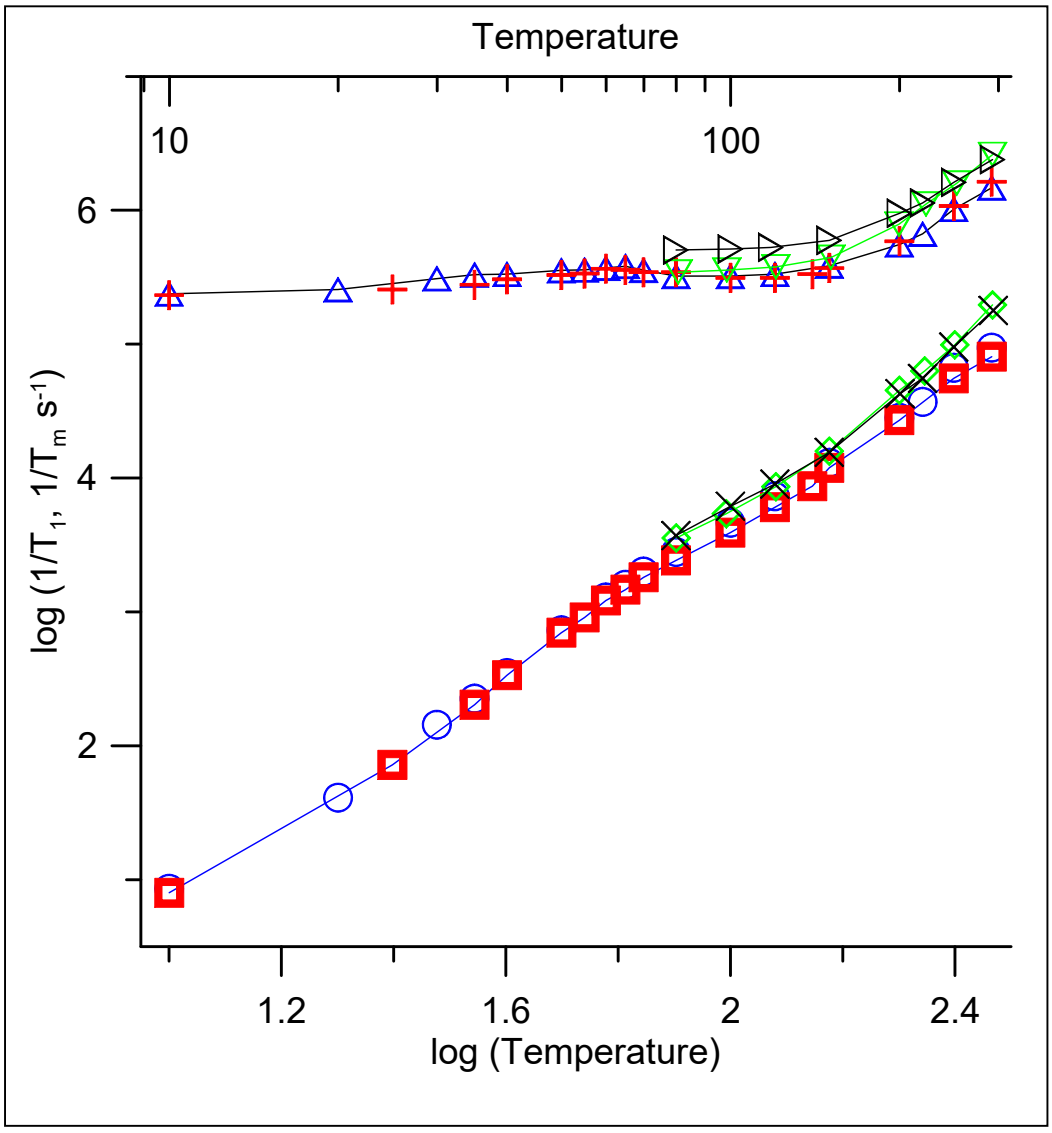
Temperature
10
100
6
4
2
log (1/T1, 1/Tm s-1)
1.2
1.6
2
2.4
log (Temperature)

Figure 6.

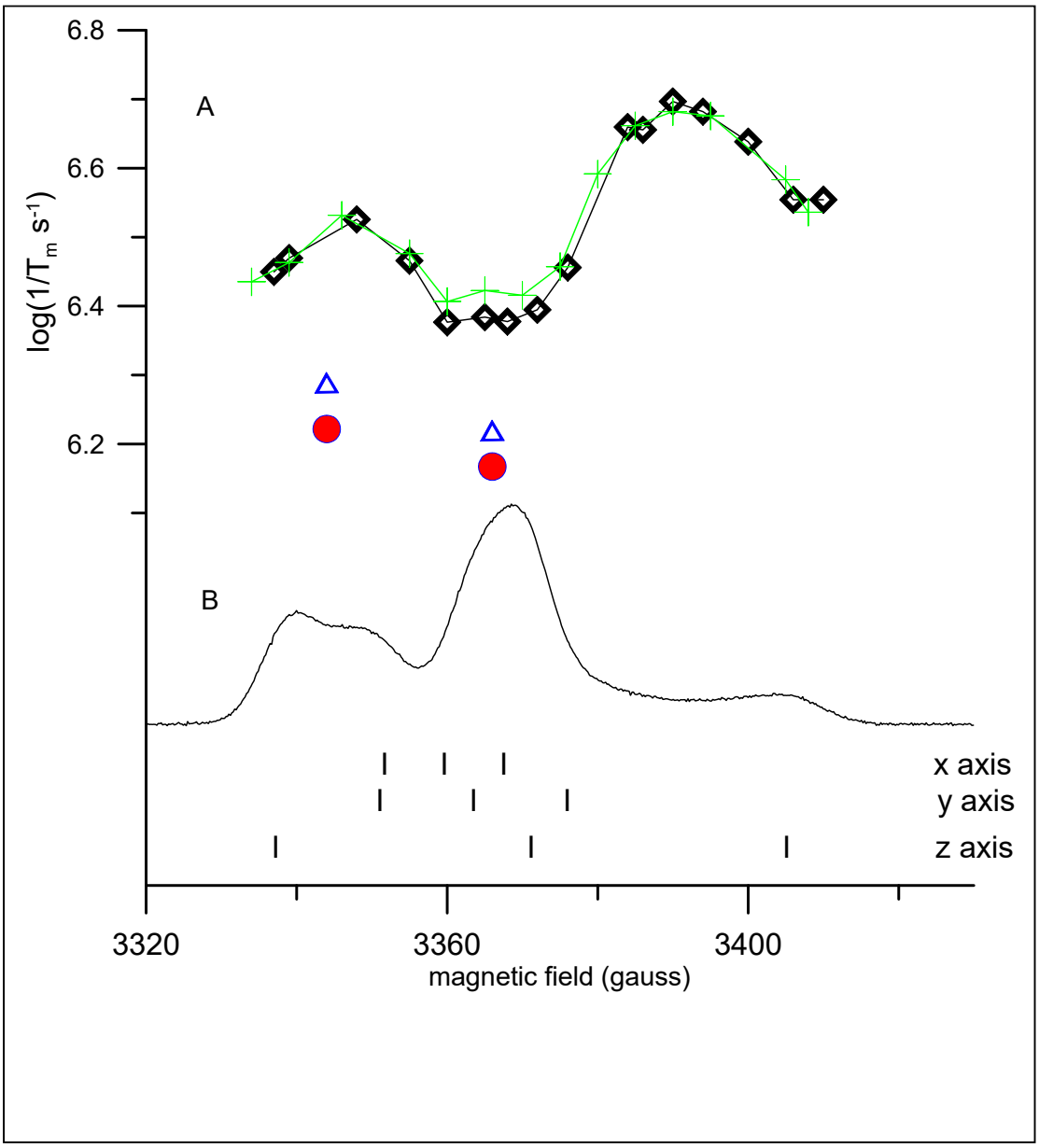
6.8
6.6
6.4
6.2
log(1/T$_m$ s^{-1})
A
B
x axis
y axis
z axis
3320
3360
3400
magnetic field (gauss)